Eur. Phys. J. A **2**, 295–300 (1998)

THE EUROPEAN PHYSICAL JOURNAL A

Production of fragments with $Z \geq 8$ in interaction of 12.7 GeV ^{4}He+U, Pb, Au and Ag: track detector study

Ž. Todorović[1], S. Savović[2], S. Jokić[3]

[1] Institute of Physics, P. O. Box 68, 11080 Belgrade, Yugoslavia
[2] Faculty of Science, P. O. Box 60, 34000 Kragujevac, Yugoslavia
[3] Institute of Nuclear Sciences "Vinča", 11101 Belgrade, Yugoslavia

Received: 28 November 1997 / Revised version: 24 April 1998
Communicated by B. Povh

Abstract. The processes of production of fragments with $Z \geq 8$ in the interaction of 12.7 GeV ^{4}He with U, Pb, Au and Ag have been analyzed using the polycarbonate track detector Makrofol. The sandwich technique was used which enables direct observation of multiply charged fragment emission by a single nucleus. The decay channels ending with one, two, or more (three, four) fragments were detected. A classification scheme based on the multiplicity of heavy fragments with $Z > 20$ was used in order to identify the events belonging to the different reaction channels. The cross sections, excitation energies and multiplicities of intermediate-mass fragments $8 \leq Z \leq 20$ have been determined for the various reaction mechanisms, and their variation as a function of the target mass has been investigated.

PACS. 25.55.-e ^{3}H-, ^{3}He-, and ^{4}He-induced reactions – 25.70.P$_2$ Multifragment emission and correlations – 25.85.Ge Charged-particle-induced fission

1 Introduction

In the light-ion-induced reactions, during the fast cascade process, the residual nuclei with a wide mass and excitation energy distributions are formed. Decay of the target residue is a field of intensive both theoretical and experimental study. Recently, a number of papers have been devoted to the investigation of the reactions using different light-ion-target combinations at different energies, providing an important insight into the competition between the mechanisms involved over the full range of internal excitations [1–6]. Excitation energy per nucleon is an important parameter governing the decay mode of the residual nuclei. In peripheral interactions of a projectile with a target, the residual nuclei sustaining small excitation energies ($E_x \leq 2$ MeV/u), decay via emission of light particles (n, p, α) and binary fission. In the first type of the process, after emission of light particles, heavy fragments with masses close to the target mass are produced. In the second type of the process, two fragments with masses of about half of the target mass are emitted. The residual nuclei with excitation energies equal to, or greater than the binding energy of the nucleus, completely decay via emission of nucleons and complex particles. Between these two boundaries of excitation energies, the decay of the residual nuclei via emission of intermediate-mass fragments (IMF: $3 \leq Z \leq 20$) is a dominant decay channel [1–9]. In this domain of excitation energies production of one and two fragments in the fission mass region is registered, in coincidence with large multiplicity of fast light charged particles [8, 10, 11].

In studying nuclear fragmentation processes, it is necessary to separate the contributions of a different mechanisms, on the basis of correlation measurements of the certain parameters of the reaction products (the angular range, the velocity and mass of fragments, etc.). In our experiment a polycarbonate track detector was used in the sandwich technique. This enabled the correlative measurements of the reaction products with atomic number $Z \geq 8$ in (almost) 4π geometry. In order to identify the events belonging to the different reaction channels, a classification scheme based on the multiplicity of heavy fragments with $Z > 20$ was used. In this experiment we have analyzed reaction mechanisms which led to production of fragments with masses in the range of fission product masses and intermediate-mass fragments $8 \leq Z \leq 20$.

2 Experimental method

The detectors used in this experiment consisted of two Makrofol foils of the size $(40 \times 30 \times 0.2)$ mm^3 in the form of a sandwich. The targets were evaporated under high vacuum directly on one of the foils. Another foil of the same dimension was pressed and partially glued to the first one. The target layer being thus enclosed between the two detector sheets. The target thickness varied from

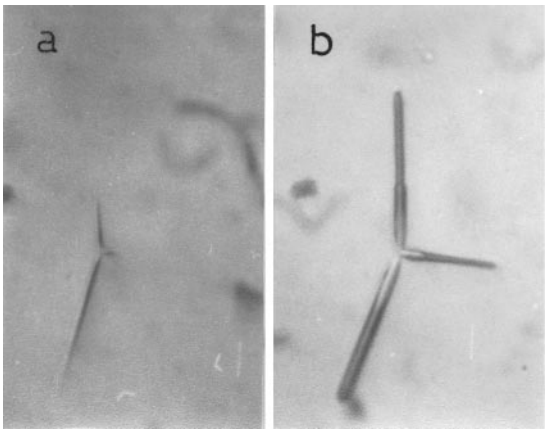

Fig. 1. Event with two IMF's and one heavy fragment (12.7 GeV ^{4}He+Au) **a** after the first etching **b** after the second etching

stack to stack between 10 and 130 μg/cm^2 and it was determined with an accuracy to within 10 %. The targets were exposed at normal incidence with 12.7 GeV alpha particles of the Synchrophasotron at Dubna (Russia). The integrated flux was $8{\cdot}10^{10}$ alpha particles and it was confined to an area (30×20) mm^2. The error in the flux determination was about 10 %. After exposition, the target was removed by dissolving it in an appropriate acid and the detector was etched two times in 20 % NaOH at 60°C within ultrasound field. The duration of the first etching was 25 min. After that the detector was rinsed in water during 20 min. and in alcohol for 10 min. within ultrasound field and etched again for 75 min. For IMF's $8 \leq Z \leq 20$ and $10 < REL < 23$ MeV mg^{-1}cm^2, where REL denotes Restricted Energy Losses, the difference between the track portions etched during the first and the second phase of etching is visible, and the parameters for the identification of the fragments (mean track etch rate and the total range) are easy to measure. In this way we could identify the charge of the IMF's with charge resolution $\Delta Z \leq 1$ [12, 13]. In Fig. 1 we present an event with two IMF's and one heavy fragment, produced in the interaction of 12.7 GeV ^{4}He with Au, after the first and after the second etching. The difference between the track portion developed during the first versus second etching is evident for IMF. The heavy fragment tracks could easily be recognized because of their high etch rate. They are mostly completely developed during the first etching. In order to identify heavy fragments we applied empirical energy-range $E = f(R)$ and mass-range $A = f(R, E)$ relations given in [13]. The upper limit of uncertainty of determination of mass was approximately up to 10 u and for determination of energy, approximately up to 10 MeV.

The detector scanning and the measurement of the track parameters were performed by the optical microscope with magnifications 300 × and 900 ×, respectively. We lost the tracks of the fragments due to the absorption in the target layer, the critical angle and the distortion of the tracks near the surface of the detector. The loss of the fragments being the function of their track lengths in the detector (which depend on the charge Z and energy E of the fragment) and angles with respect to the beam. Using the actual distribution of the track lengths and the isotropical angular distribution, the estimated detection efficiency was 90–95 % for heavy fragments and 80–90 % for intermediate-mass fragments.

The following types of events were found: (i) Events with a single track that can not be coupled with any other track in the detector, (ii) Events with two, three and four tracks belonging to the fragments from the same interaction. The criterion used for the identification of these events was that the tracks of emitted fragments should intersect in the plane of the target. The coincidences of two single tracks or of a single track and a binary events may lead to false binary or ternary events, respectively. The coincidence of individual types of events is strongly dependent upon their density in the detector. The percentage of double and triple accidental coincidences was found to be (0.05–0.2)% and (2–5)% of the observed number of binary and ternary events, respectively.

3 Results and discussion

The fragments produced in our experiment were identified and an event-by-event model-free analysis was performed. The various mechanisms contribute to the production of events. On the basis of the multiplicity of heavy fragments M_H, we classified the events into the following reaction channels: fission ($M_H = 2$), spallation ($M_H = 1$) and multifragmentation ($M_H = 0$) [8, 9]. A boundary between heavy and intermediate-mass fragments lies around $Z = 20$ [9]. The multiplicity of IMF's with charge $8 \leq Z \leq 20$ in these events varied from $M_{IMF} = 0$ to $M_{IMF} = 3$. In Table 1 is given the number of events studied in the different event categories and the total number of events for all the analyzed targets.

Table 1. The number of events studied in the different event categories and the total number of events for all the analyzed targets

	U	Pb	Au	Ag
$M_H = 0$	344	604	742	589
$M_H = 1$	1214	1474	1579	1780
$M_H = 2$	4278	1188	1168	231
Total	5836	3266	3489	2600

3.1 Production of heavy fragments ($Z > 20$)

According to the classification scheme given above, heavy fragments can be produced in the process of fission and spallation. In the light-ion-induced reactions, the three different fission mechanisms are registered on the basis of the measurements of multiplicity of fast nucleons and the yield of IMF's produced in correlation with two heavy fragments [1, 2, 4, 7, 8, 10, 14]. One of them is binary

fission. In the binary fission process two heavy fragments are produced, in correlation with a small number of fast nucleons. For the light-ion-induced reactions, the number of fast nucleons does not exceed twice the projectile mass number [1]. From the systematics of momentum transfer to the fissioning residue in high-energy light-ion collisions, there is a strong evidence that binary fission is predominantly associated with peripheral collisions [1, 8, 10]. The second mechanism is violent, i.e. it appears in coincidence with a number of fast nucleons and several light charged particles [10, 14]. In this type of fission process, fragments with smaller mass and larger kinetic energy are produced, in comparison to the binary fission [14]. Such a process has been interpreted as a kind of cleavage: the projectile drills a hole through the target and the system breaks into two pieces [8, 14, 15]. The third mechanism is related to the production of two heavy fragments in coincidence with IMF [2, 4, 7]. IMF's are predominantly produced in the fragmentation processes of the residual nucleus in the central collisions and these processes differ from the processes which are responsible for the emission of fast nucleons and light charged particles. Namely, the most of the light charged particles, like nucleons, originate from other processes not related to the fragmentation of the residual nucleus (contributions from ejectiles emitted during the fast cascade/nonequilibrium stages of the reaction, coalescence involving fast cascade nucleons which may produce significant yields of nonequilibrium light particles, evaporation [5, 8, 11]). In earlier works [2, 4] it is shown that IMF emission occurs prior to fission and the average number of IMF's emitted per such fragmentation event is close to unity.

We can easily identify the binary fission events using the correlation between the common observables which characterize fission events. From our complete binary measurements we can construct the relative velocity v_{ij} of the fissioning fragments in the rest frame of the fissioning system and then compare to known systematics for low-energy fission [16]. As known from Viola systematics, binary fission of an equilibrated nucleus leads to a small range of relative velocities between the fragments, nearly independent of the mass of the fissioning nucleus. In order to distinguish the binary fission events from the events $M_H = 2$, $M_{IMF} = 0$, where two heavy fragments are produced in other inelastic processes, we used the dependence $v_{ij}(\Delta A)$, where ΔA is defined as a difference between the target mass and the sum of the heavy fragment masses. From Fig. 2, where we display the function $v_{ij}(\Delta A)$ in case of 12.7 GeV ^{4}He+Au interaction, one can observe two clearly separated groups. For all events with $\Delta A < 40$, a narrow distribution of relative velocities is centered at a value which corresponds to Viola systematics [16] characterizing binary fission processes. In Table 2 are given the mean values of ΔA, the linear momentum transfer $p_\parallel$ and the cross sections for the binary fission events for all the analyzed targets. The values of ΔA represent a measure of the excitation energy of the residual nuclei, since in binary fission process only a small number of fast nucleons is produced. With decreasing target mass

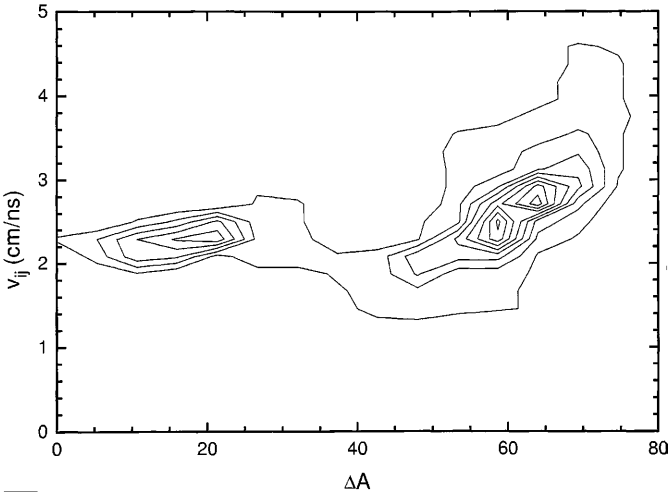

Fig. 2. Contour plot of the relative velocity between fragments from $M_H = 2$, $M_{IMF} = 0$ events as a function of mass loss for the 12.7 GeV ^{4}He+Au reaction

Table 2. Mean values of mass losses ΔA, linear momentum transfers $p_\parallel$ and cross sections σ_{bf} for binary fission events

Target	$< \Delta A >$	$< p_\parallel >$ (MeV/c)	σ_{bf} (mb)
U	16 ± 5	204 ± 65	940 ± 95
Pb	18 ± 6	412 ± 135	95 ± 20
Au	21 ± 6	505 ± 154	65 ± 14
Ag	24 ± 8	1343 ± 495	2 ± 0.8

$< \Delta A >$ increases and reflects the relative importance of the different fragmentation processes with higher excitation energies. The values of the linear momentum transfer are determined by measuring the angles of both fragments with respect to the beam direction as well as the velocities of the fragments [1]. The results show a strong correlation between the linear momentum transfer and $< \Delta A >$. With decreasing target mass, the mean values of the linear momentum transfer of the fissioning nuclei and $< \Delta A >$ are larger, reflecting the subgroups of the collisions with higher excitation energies selected by higher fission barriers.

In Fig. 2 we see that for larger values of ΔA, the mean value of relative velocity starts to shift towards larger values, and the distribution starts to broaden significantly. This might be due to the emission of number of nucleons and several light charged particles (violent fission) as well as the emission of IMF with $Z < 8$, but the present experiment can not distinguish between these two mechanisms. These events together with the events in which in addition to the two heavy fragments at least one IMF $8 \leq Z \leq 20$ is registered, form a group of fission-like events. In the interaction of 12.7 GeV ^{4}He with U, Pb and Au we registered 6 %, 16 % and 18 %, respectively, of the fission-like events where besides the two heavy fragments at least one IMF $8 \leq Z \leq 20$ is registered.

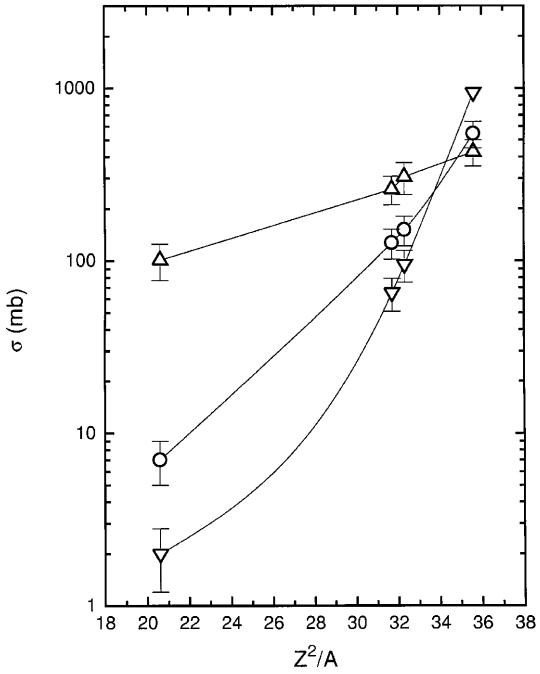

Fig. 3. Cross sections for production of events with heavy fragments as a function of target parameter Z^2/A for [▽] binary fission, [○] fission-like and [△] deep spallation and associated spallation events

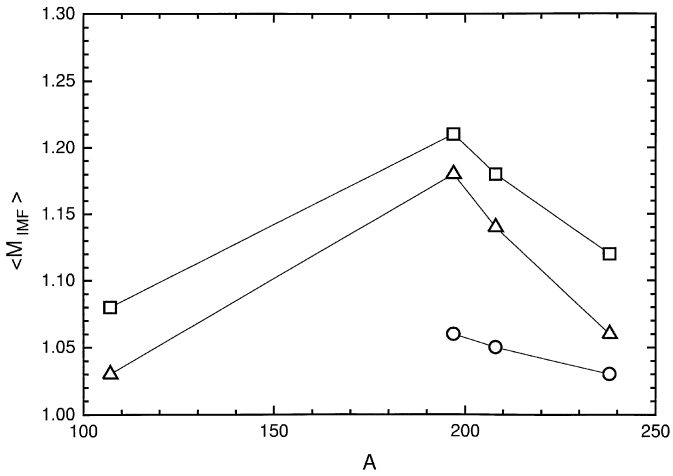

Fig. 4. Mean multiplicity of IMF's $8 \leq Z \leq 20$ as a function of target mass for [○] fission-like, [△] associated spallation and [□] multifragmentation events. Statistical errors are estimated to be ±25%

In the previous experiments it appeared that the events with one heavy fragment could be produced in the peripheral and the central collisions of a projectile with a target [3, 7–9, 11]. In the peripheral interactions after emission of light particles, a fragment with mass $A \geq \frac{2}{3} A_t$, where A_t is the target mass, and with mean kinetic energy $< E_k >= \epsilon_s(A_t - A)/A_t$, where ϵ_s=10–20 MeV, is produced [8]. By using the energy-range dependence for these fragments in Makrofol [13,17], we see that their range is $R \leq 5$ μm. In this paper these single fragments have not been analyzed. The unpaired single heavy fragments with range $R > 5$ μm are attributed mainly to the very energetic spallation residues. In earlier experiments it is shown that these fragments can be produced in the processes of deep spallation and associated spallation [3, 7–9, 11]. In deep spallation processes a heavy fragment is produced in coincidence with large multiplicity of the fast light particles and its mass is in the domain of the masses of the fragments produced in the binary fission process [8,11]. In associated spallation processes a heavy fragment is emitted in coincidence with one or more IMF [3,7,9]. In the interaction of 12.7 GeV ^{4}He with U, Pb, Au and Ag we registered 27 %, 37 %, 39 % and 13 % of events, respectively, where besides one heavy fragment at least one IMF $8 \leq Z \leq 20$ is registered. Such an event in which besides one heavy fragment two IMF's are registered is shown in Fig. 1.

The measured cross sections for different reaction channels in which heavy fragments are produced, as a function of the target parameter Z^2/A, are shown in Fig. 3. The errors presented in Fig. 3 are due to the statistical fluctuations and the scanning errors, the uncertainties in the thickness of the target layers and the errors in the integrated fluxes. The cross section for binary fission increases rapidly with the parameter Z^2/A, following the decrease of the fission barrier and becoming a dominant process for interaction with U. The cross section for production of the events in the fission-like process increases rather slowly with the parameter Z^2/A, in comparison to the increase of the cross section for the binary fission. Deep spallation and associated spallation processes are dominant for the targets lighter than U, but the increase of the cross section with increasing target mass is not as rapid as the increase of the cross section for fission.

3.2 Production of IMF's ($8 \leq Z \leq 20$)

In the high energy nuclear interactions the following three mechanisms contribute to the production of IMF's over the whole range of the excitation energy of the residual nuclei: multifragmentation, associated spallation and fission following IMF emission [2–9]. Decay channels of the residual nucleus depend essentially on its excitation energy per nucleon [7]. Several experimental variables are closely correlated with the excitation energy. These include the observed multiplicity M_{IMF} of IMF's, Z_B (the sum of the charges of all fragments with $Z \geq 2$, in our experiment $Z \geq 8$) and the parallel residual velocities [5, 7, 18]. The mean IMF multiplicity increases with increasing excitation energy, at least up to the high excitation energy which characterizes multifragmentation [18]. In Fig. 4. we give the mean multiplicity of IMF's as a function of the target mass for the three different event classes where at least one IMF is registered. The mean IMF multiplicities for the events produced in the processes of multifragmentation and associated spallation are changing as a function of the target mass in a similar manner. The largest values of the multiplicity of IMF's are obtained for

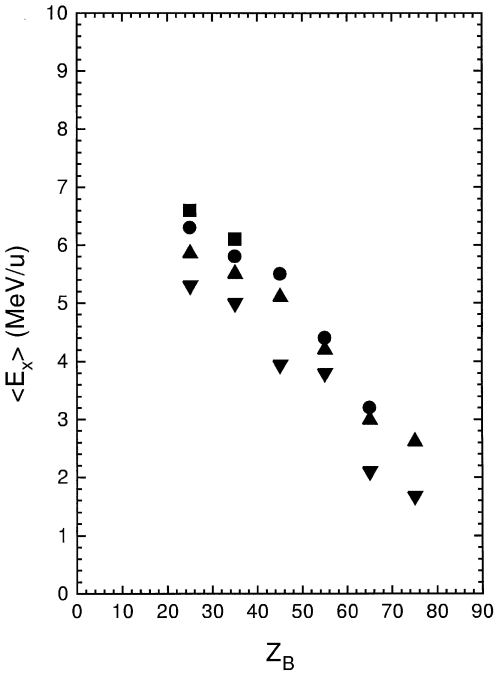

Fig. 5. Mean excitation energy of the decaying residual nucleus as a function of Z_B for the interactions of 12.7 GeV ^{4}He with [▼] U, [▲] Pb, [●] Au and [■] Ag

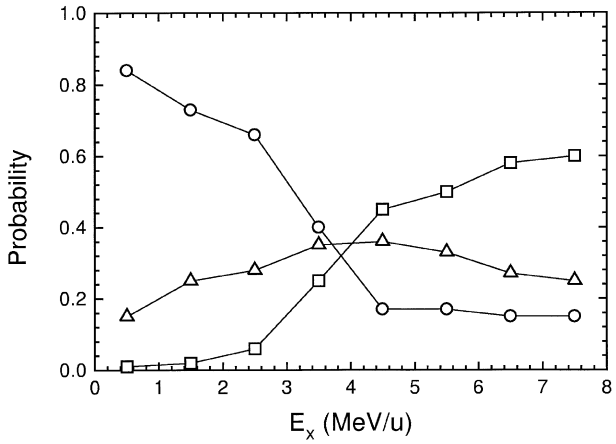

Fig. 6. Evolution of the probabilities for three different event categories as a function of excitation energy per nucleon for [○] fission-like, [△] associated spallation and [□] multifragmentation events for the 12.7 GeV ^{4}He+U reaction

the events produced in the process of multifragmentation, while the smallest obtained multiplicities of IMF's characterize fission-like processes for all the analyzed targets. In the high-energy light-ion collisions the fragments originate from the decay of the target residue and then its velocity is determined by $\mathbf{v}_R = \sum_i A_i \mathbf{v}_i / \sum_i A_i$, where A_i is the fragment mass and $\mathbf{v}_i$ is the fragment velocity in the laboratory system (the sum runs over all detected fragments originated from a single source). At these beam energies the relation between parallel residual velocity v_R^{par} (the projection of the velocity of the target residue $\mathbf{v}_R$ along the beam axis) and excitation energy E_x is preserved [8]. To estimate the excitation energy of the target residue we used the simple formula [7] $E_x = \frac{1}{2} m_n \mathrm{v}_R^{par} (\mathrm{v}_{beam} - \mathrm{v}_R^{par})$, where m_n is the nucleon rest mass. The main assumption which makes this formula useable at such high energy is that all projectile-like particles (*p, d, t,* ^{3}He) are emitted in the beam direction with the beam velocity v_{beam}. Such processes are dominant in the high-energy light-ion induced reactions [19]. In our work, due to the failure to detect, and therefore, to account for preequilibrium particle emission and for IMF's with $Z < 8$, the excitation energy may be in error by up to 30%, but such errors should only compress the energy scale (nearly equal for all the analyzed processes) and not destroy the simple pattern that is observed in the data. In Fig. 5 are given the estimated mean excitation energies per nucleon as a function of Z_B. For all the analyzed targets, the excitation energy per nucleon of the residual nuclei is nearly linearly increasing with decreasing Z_B. Due to the tracking threshold $Z \geq 8$ of the detector, this investigation is limited over the range $Z_B \approx 20$ to 80. The majority of the events produced in multifragmentation, associated spallation and fission-like processes have Z_B in the interval 20 to 40, 40 to 60 and 60 to 80, respectively.

In order to obtain a more complete picture of the influence of the excitation energy in the production of IMF's, we determined the evolution of the probabilities for the three different event categories as a function of the excitation energy per nucleon for 12.7 GeV ^{4}He+U interaction, given in Fig. 6. On the basis of the obtained results, we see that the fission-like events are mostly produced in the decay process of the residual nuclei with the excitation energies smaller than ≈ 3 MeV/u. Associated spallation events are produced in the process of the decay of the residual nuclei with rather broad range of excitation energy with a weakly pronounced maximum of the probability at about 4 MeV/u. The dominant decay mode of the residual nuclei with the excitation energies greater than ≈ 5 MeV/u is multifragmentation. These results are consistent with other recent measurements [7, 20].

Evolution of the probabilities for the three event categories in which at least one IMF is registered, as a function of the target mass is shown in Fig. 7. It can be seen that processes of multifragmentation and associated spallation are dominant for production of events with IMF in the interaction of ^{4}He with heavier targets, while for the lighter nuclei, such as Ag, the dominant process is multifragmentation. In order to make more meaningful comparison between the four targets, a scaling the upper threshold for IMF's with the maximum mass of the system has been done. No noteworthy difference is observed, i. e. the exact location of our upper threshold for IMF's ($Z \leq 20$) does not crucially affect this comparison of probabilities. Such behaviour of the probabilities for production of IMF is a consequence of the influence of excitation energy per nucleon deposited in the residual nuclei. For fixed beam energy the mean values of excitation energies per nucleon of the residual nuclei increase with decreasing target mass [5]. The

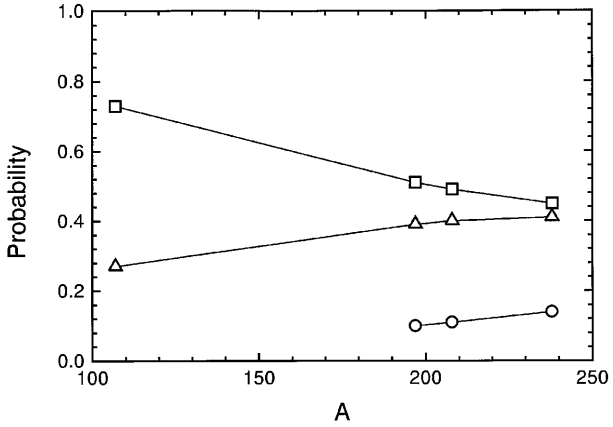

Fig. 7. Evolution of the probabilities for production of events in which at least one IMF $8 \leq Z \leq 20$ is emitted as a function of target mass for [○] fission-like, [△] associated spallation and [□] multifragmentation events

probability of the production of events with two heavy fragments in correlation with IMF is small and decreases rather slowly with decreasing target mass. This can be explained by the fact that after the emission of IMF $8 \leq Z \leq 20$ and a number of nucleons, the residual nuclei in the domain of the light nuclei are produced, for which fission probability is small and does not depend on the parameter Z^2/A, but depends on the excitation energy [8].

4 Conclusion

We have studied the production of heavy fragments in the fission mass region and IMF's $8 \leq Z \leq 20$ in the interaction of 12.7 GeV ^{4}He with U, Pb, Au and Ag. From the complete measurements of the resulting target fragments with $Z \geq 8$ we have observed the different mechanisms which contribute to the production of the analyzed fragments. The cross sections for the various reaction channels as a function of the target mass are analyzed. The results show that in the interaction of 12.7 GeV ^{4}He with heavy nuclei, such as U, the dominant process in the production of heavy fragments is fission (binary fission, violent fission and fission following IMF emission). For nuclei lighter than U the dominant processes in the production of heavy fragments are deep spallation and associated spallation. The processes of multifragmentation and associated spallation are dominant in the production of IMF's $8 \leq Z \leq 20$ in the interaction of 12.7 GeV ^{4}He with U, Pb and Au, while for the lighter nuclei, such as Ag, the dominant process is multifragmentation.

We are grateful to Profs. A.M. Baldin and I.N. Semenyushkin for the exposure of the detectors and for measurement of the flux. We are also thankful to the technical staff of our Laboratory for accurate measurements.

References

1. Klotz-Engmann, G., Oeschler, H., Stroth, J., Kankeleit, E., Cassagnou, Y., Conjeaud, M., Dayras, R., Harar, S., Legrain, R., Pollacco, E.C., Volant, C.: Nucl. Phys. A**499**, 392 (1989)
2. Fatyga, M., Byrd, R.C., Kwiatkowski, K., Wilson, W.G., Woo, L.W., Viola Jr., V.E., Karwowski, H.J., Jastrzebski, J., Skulski, W.: Phys. Lett. B**185**, 321 (1987)
3. Grabež, B., Gerc, V.: Phys. Lett. B**207**, 27 (1988)
4. Lips, V., Barth, R., Oeschler, H., Avdeyev, S.P., Karnaukhov, V.A., Kuznetsov, W.D., Petrov, L.A., Bochkarev, O.V., Chulkov, L.V., Kuzmin, E.A., Karcz, W., Neubert, W., Norbeck, E.: Phys. Rev. Lett. **72**, 1604 (1994)
5. Morley, K.B., Kwiatkowski, K., Bracken, D.S., Renshaw Foxford, E., Viola, V.E., Woo, L.W., Yoder, N.R., Legrain, R., Pollacco, E.C., Volant, C., Korteling, R.G., Breuer, H., Brzychczyk, J.: Phys. Rev. C**54**, 737 (1996)
6. Renshaw Foxford, E., Kwiatkowski, K., Bracken, D.S., Morley, K.B., Viola, V.E., Yoder, N.R., Volant, C., Pollacco, E.C., Legrain, R., Korteling, R.G., Friedman, W.A., Brzychczyk, J., Breuer, H.: Phys. Rev. C**54**, 749 (1996)
7. Bizard, G., Bougault, R., Brou, R., Colin, J., Durand, D., Genoux-Lubain, A., Laville, J.L., Le Brun, C., Lecolley, J.F., Louvel, M., Péter, J., Steckmeyer, J.C., Tamain, B., Badala, A., Motobayashi, T., Rudolf, G., Stuttgé, L.: Phys. Lett. B**302**, 162 (1993)
8. Hüfner, J.: Phys. Rep. **125**, 129 (1985)
9. Lewenkopf, C., Dreute, J., Abdul-Magd, A., Aichelin, J., Heinrich, W., Hüfner, J., Rusch, G., Wiegel, B.: Phys. Rev. C**44**, 1065 (1991)
10. Meyer, W.G., Gutbrod, H.H., Lukner, Ch., Sandoval, A.: Phys. Rev. C**22**, 179 (1980)
11. Warwick, A.I., Wieman, H.H., Gutbrod, H.H., Maier, M.R., Péter, J., Ritter, H.G., Stelzer, H., Weik, F., Freedman, M., Henderson, D.J., Kaufman, S.B., Steinberg, E.P., Wilkins, B.D.: Phys. Rev. C**27**, 1083 (1983)
12. Todorović, Ž., Antanasijević, R.: Nucl. Instr. and Meth. **212**, 217 (1983)
13. Lazić, D.L., Todorović, Ž.: Nucl. Instr. and Meth. B**61**, 239 (1991)
14. Wilkins, B.D., Kaufman, S.B., Steinberg, E.P., Vrbon, J.A., Henderson, D.J.: Phys. Rev. Lett. **43**, 1080 (1979)
15. Wang, G., Kwiatkowski, K., Viola, V.E., Bauer, W., Danielewicz, P.: Phys. Rev. C**53**, 1811 (1996)
16. Viola, V.E., Kwiatkowski, K., Walker, M.: Phys. Rev. C**31**, 1550 (1985)
17. Tripier, J., Remy, G., Ralarosy, J., Debeauvais, M., Stein, R., Huss, D.: Nucl. Instr. and Meth. **115**, 29 (1974)
18. Hubele, J., Kreutz, P., Adloff, J.C., Begemann-Blaich, M., Bouissou, P., Imme, G., Iori, I., Kunde, G.J., Leray, S., Lindenstruth, V., Liu, Z., Lynen, U., Meijer, R.J., Milkau, U., Moroni, A., Müller, W.F.J., Ngô, C., Ogilvie, C.A., Pochodzalla, J., Raciti, G., Rudolf, G., Sann, H., Schüttauf, A., Seidel, W., Stuttgé, L., Trautmann, W., Tucholski, A.: Z. Phys. A**340**, 263 (1991)
19. Belaga, V.V., Bondarenko, A.I., Kanarek, T., Karshiev, D.A., Kladnitskaya, E.N., Kuznetsov, A.A., Togoo, R., Toneeva, G.P., Chernov, G.M., Yuldashev, B.S.: Phys. Atom. Nucl. **59**, 1935 (1996)
20. Li, Bao-An., Gross, D.H.E., Lips, V., Oeschler, H.: Phys. Lett. B**335**, 1 (1994)